Check for updates

How to cite: *Angew. Chem. Int. Ed.* **2023,** *62,* e202300785
International Edition: doi.org/10.1002/anie.202300785
German Edition: doi.org/10.1002/ange.202300785

Heterocycles

Diazadiboraacenes: Synthesis, Spectroscopy and Computations

*Julia Ruhl, Nils Oberhof, Andreas Dreuw, and Hermann A. Wegner**

Abstract: The incorporation of heteroatoms into hydrocarbon compounds greatly expands the chemical space of molecular materials. In this context, B–N doping takes a center stage due to its isosterism with a C=C-bond. Herein, we present a new and modular synthetic concept to access novel diazadiborabenzo-[*b*]triphenylenes **7a–h** using the B–N doped biradical **16** as intermediate. Characterization of the photophysical properties revealed the emission spectra of the diazadibora benzo[*b*]triphenylenes **7a–h** can conveniently be tuned by small changes of the substitution on the boron-atom. All of the diazadibora compounds show a short life-time phosphorescence. Additionally, we were able to rationalize the excited-state relaxation of the diazadiboraacene **7a** via intersystem crossing by quantum chemical calculations. The new synthetic strategy provides an elegant route to various novel B–N doped acenes with great potential for applications in molecular materials.

Polycyclic aromatic hydrocarbons (PAHs) have received noteworthy attention in materials research due to their application potential, e.g. in organic light emitting diodes (OLEDs),[1] organic field-effect transistors (OFETs),[2] or solar cells.[3] This is *inter alia* related to their versatile structure dependent properties and their modular synthetic access.[4] Further, the implementation of boron in PAHs was shown to lead to new exceptional optoelectronic materials.[5,6] By introducing one boron and one nitrogen next to each other in PAHs, the resulting compounds are isosteric and isoelectronic to the all-carbon analogue (B–N/C=C isosterism). This does however introduce, a dipole moment in the PAH, which can significantly influence the solid-state structure as well as electronic and optoelectronic properties but the existing molecular structural features are maintained. These changes are due to the modification of the gap between the highest occupied and lowest unoccupied molecular orbital (HOMO and LUMO), as well as the intermolecular interactions in the solid state.[5,7]

Pioneers of this concept were Dewar et al.,[8] who already presented the synthesis of various diazadibora-analogues of pyrene and anthracene **1** in the 1950s and 1960s (Figure 1).[9] In addition, they also presented the synthesis of azabora-naphthalene and phenanthrene, in which the isoelectronic B–N moieties replaced C=C positions at the perimeter of the compounds. Notwithstanding of the useful properties of B,N doped acenes and their role in PAH chemistry, it took over 50 years until parental BN isosteres of higher acenes, besides the bicyclic naphthalene, have been reported.[10] For example, in 2014 Chrostowska and co-workers showed a new synthesis to implement B–N moieties in anthracene systems and the properties of these B,N-anthracenes **2**.[11] In 2021, Tian et al. reported a novel synthesis of 9,9a-B,N anthracene derivatives **3** along with its photophysical properties.[12]

In most cases of B,N-PAHs the B–N units are spatially separated by multiple carbon bonds. In this way, separated polar bonds are implemented in the molecules leading mostly to a weak additional dipole moment. However, when the two B–N bonds are, connected via the N-atoms, in the molecular structure, the combined polar bonds should lead to a stronger overall dipole moment of the molecule. The first synthesis of such diazadiboracenes were reported by Siebert and co-worker with the example of the 2,3,1,4-diazadibora naphthalenes **4** in 1978.[13] Piers and co-workers

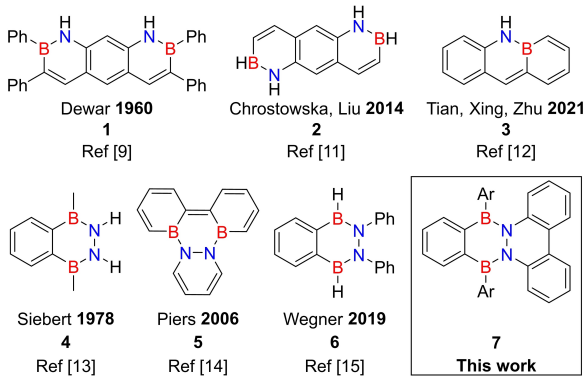

Figure 1. Selection of six-membered BN isosteres of anthracene and BN isosteres of PAHs with a $C_2B_2N_2$ core.

[*] J. Ruhl, Prof. Dr. H. A. Wegner
Institute of Organic Chemistry, Justus Liebig University Giessen
Heinrich-Buff-Ring 17, 35392 Giessen (Germany)
and
Center for Materials Research (LaMa), Justus Liebig University Giessen
Heinrich-Buff-Ring 16, 35392 Giessen (Germany)
E-mail: Hermann.A.Wegner@org.chemie.uni-giessen.de
N. Oberhof, Prof. Dr. A. Dreuw
Interdisciplinary Center for Scientic Computing, Heidelberg University
Im Neuenheimer Feld 205, 69120 Heidelberg (Germany)

© 2023 The Authors. Angewandte Chemie International Edition published by Wiley-VCH GmbH. This is an open access article under the terms of the Creative Commons Attribution Non-Commercial License, which permits use, distribution and reproduction in any medium, provided the original work is properly cited and is not used for commercial purposes.

© 2023 The Authors. Angewandte Chemie International Edition published by Wiley-VCH GmbH

reported the same pattern incorporated inside a triphenylene unit.[14,15] They investigated the synthesis and the photophysical properties of diazadiboratriphenylene **5**. By introducing different diazines to their boron precursor they were able to alter the photophysical and electronic properties of these compounds. In addition, they observed short B••N intermolecular coordination in crystal structure. This strengthened the (π)-stacking of the triphenylene **5**, which could lead to better electron transport in electronic materials.

Recently, our group reported a synthetic route to diazadiboranaphthalenes **6** and investigated their photophysical properties.[16] In these studies, we were able to show that the diazadiboranaphthalenes **6** exhibits two solvent-dependent emissions, and the one at longer wavelength was attributed to a twisted intramolecular charge transfer (TICT). This TICT behavior was supported by computations and matrix-isolation experiments. Furthermore, in 2017 we showed the synthesis and properties of a B,N-based stable biradical **16**.[17] Interestingly, we could demonstrate by ^{1}H NMR spectroscopy that in the presence of a competing ligand, such as pyridine, the second coordination of the benzo[*c*]cinnoline (**15**) is reversible in solution and in equilibrium with pyridine. However, the diazadiborabenzo-[*b*]triphenylene backbone was only observed spectroscopically and could not be isolated.

Herein, we present the preparation and investigation of novel diazadiborabenzo[*b*]triphenylenes **7a**–**h**. We started first with the synthesis goal of an air-stable diazadibora benzo[*b*]triphenylene. In general, there are two possible strategies to stabilize a trivalent boron in PAHs. The first one is the "principle of structural constraint".[18] In this approach, the boron is stabilized by embedding it into the inner part of PAHs. As a result, tetra-coordinated adducts of the boron become unfavorable and C–B bond cleavage is prevented by the chelating effect. The other approach method is the "principle of steric shielding".[19] Herein, bulky substituents (e.g. mesityl-groups) are attached to the boron, which leads to kinetic protection.[20] To not extend the π-system and to prevent changes to the molecular structure, we chose the method of steric shielding to stabilize the diazadiboraacene in our design.

We planned the synthesis of the mesitylated diazadibora benzo[*b*]triphenylene **7a** by firstly cutting the molecule in three synthetic parts: the diazine, the mesitylene and the boron backbone (Scheme 1). For the diazine moiety we relied on the benzo[*c*]cinnoline (**15**), which is commercially available and has been crucial in the preparation of the radical **16**. In contrast, the mesitylene part and the boron backbone have to be synthesized (Scheme 2).

For the boron backbone we chose the bis-BCl_2-benzene **10** as intermediate. Therefore, 1,2-dibromobenzene (**8**) was transformed in a Grignard reaction with Mg and TMSCl to the bis-TMS-benzene **9** in a yield of 34 % (Scheme 2).[21] For the next step, we prepared a solution of bis-TMS-benzene **9** in dry DCM under Schlenk conditions in a pressure tube. The solution was cooled down to 0 °C and treated with 1 M solution of BCl_3 in DCM, sealed and heated to 95 °C for five days.[22] After removing the solvent and distillation of the

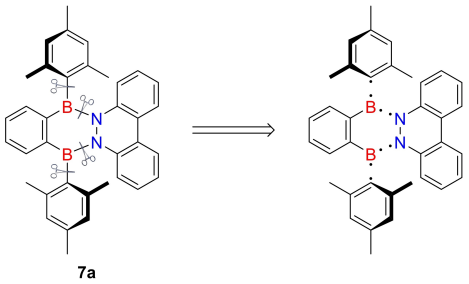

Scheme 1. Cut of the diazadiborabenzo[*b*]triphenylene **7a** in three synthetic parts.

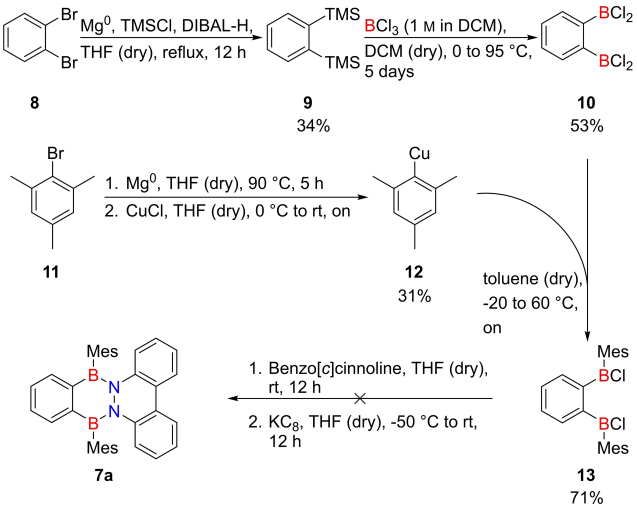

Scheme 2. Unsuccessful synthetic attempt to obtain the mesitylated diazadibora benzo[*b*]triphenylene **7a**.

crude bis-BCl_2-benzene **10** was obtained in 53 %. For the mesitylene part, copper mesitylene **12** was chosen due to its selectivity for mono-substitution on boron atoms. Compound **12** was synthesized from bromomesitylene **11** by forming the Grignard reagent in situ followed by quenching with CuCl in THF solution. This provided the copper mesitylene **12** in a yield of 31 %.[23] In the next step, the boron backbone was combined with the mesitylene part by adding the bis-BCl_2-benzene **10** to the copper mesitylene **12** in a toluene solution. After purification, the mesitylated bis-BCl-benzene **13** was isolated in a good yield of 71 %. In the last step, the benzo[*c*]cinnoline (**15**) should be added to the mesitylated bis-BCl-benzene **13** to first form the corresponding Lewis adduct and ideally after a reduction the mesitylated diazadiborabenzo[*b*]triphenylene **7a** should be obtained. Therefore, the mesitylated bis-BCl-benzene **13** and benzo[*c*]cinnoline (**15**) were stirred in THF at room temperature for 12 h. Then, KC_8 was used as reducing agent. However, the desired product **7a** was not observed.[24] In addition, the transformation was attempted with Lewis acids e.g. $AlCl_3$ but this was unsuccessful,[25] probably due to steric reasons. In an attempt to circumvent this problem, we tried to replace the chloride on the boron by a hydride using $LiAlH_4$.[26] The salt was filtered off and benzo[*c*]cinnoline

© 2023 The Authors. Angewandte Chemie International Edition published by Wiley-VCH GmbH

15213773, 2023, 15, Downloaded from https://onlinelibrary.wiley.com/doi/10.1002/anie.202300785 by Cochrane Germany, Wiley Online Library on [07/12/2023]. See the Terms and Conditions (https://onlinelibrary.wiley.com/terms-and-conditions) on Wiley Online Library for rules of use; OA articles are governed by the applicable Creative Commons License

(**15**) was added to the filtrate. Additionally, TMSCl was added to this reaction mixture to form the corresponding borane in situ. Unfortunately, in this altered approach the desired product was also not observed. Only the starting materials could be re-isolated.

As our initial strategy was not successful, we planned to establish the B–N connection of the molecule first and stabilize the scaffold afterwards by addition of the mesitylene component. We envisioned to exploit the equilibrium between the biradical **16** and **17** with respect to the coordination of a second benzo[*c*]cinnoline (**15**) (Scheme 3).[17] The synthesis commences with the preparation of lithium *o*-phenylbisborate **14** from the 1,2-dibromobenzene (**8**) via 1,2-bis(pinacolboryl)benzene according to the literature.[26] By treating the solution of lithium *o*-phenylbisborate **14** and benzo[*c*]cinnoline (**15**) with TMSCl the biradical **16** was formed, which is indicated by a dark green color. Then, the reaction mixture was treated with the mesityl Grignard reagent **18a** to capture the diazadibora unit from the equilibrium. This strategy was successful and provided the desired mesitylated diazadiborabenzo[*b*]triphenylene **7a**. During this procedure the colour of the mixture turned from dark green to dark red. After concentration, the crude product was extracted with toluene. By overlaying the yellow toluene extract with methanol, the mesitylated diazadiborabenzo[*b*]triphenylene **7a** crystallized overnight as a yellow solid in a yield of 23 %. By ^{1}H NMR experiments we could show the diazadibora **7a** to be air-stable in a THF-d_8 solution over 24 h (see Supporting Information for details). With an efficient modular synthesis approach in hand, we set out to test the scope of the strategy in terms of boron substitution. Therefore, we explored different aryl Grignard reagents **18b–h** with the same reaction set up. In this way, we could synthesize diazadibora derivatives **7b–h**. Due to their air and moisture sensitivity, they could not be purified by precipitation from the solution with methanol. The reaction mixture was therefore concentrated and the impurities were sublimated out of the crude mixture. The remaining solid was extracted with DCM and the combined extracts were concentrated under reduced pressure. In this way, the diazadiborabenzo[*b*]triphenylenes **7b–h** were obtained as pale-yellow solids in yields of 22–37 %. In a similar fashion the diaza part as well as the *o*-phenylbisborate can be altered to provide a comprehensive overview of this new class of extended B,N-PAHs, which will be part of future studies.

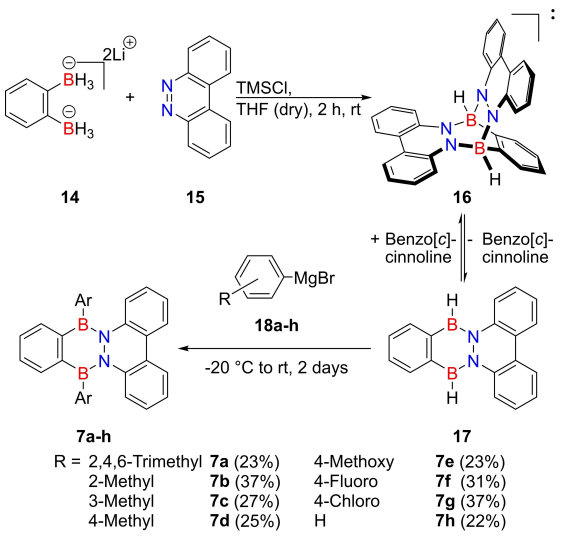

Scheme 3. Synthesis of diazadiborabenzo[*b*]triphenylenes **7a–h**, starting from lithium *o*-phenylbisborate **14** and benzo[*c*]cinnoline (**15**).

The UV/Vis spectrum of **7a** (solid black line) is shown in comparison to the spectrum of the carbon analogue, benzo[*b*]triphenylene (**19**), (solid red line) in Figure 2 (2.0×10^{-5} M in DCM). One of the absorption maxima of **7a** is blue-shifted ($\lambda_{max}=248$ nm) and the other maxima is red-shifted ($\lambda_{max}=350$ nm) in comparison to the benzo[*b*]triphenylene (**19**) ($\lambda_{max}=277$ & 289 nm). Additionally, we also investigated the absorption spectrum in THF and *n*-hexane, which resulted in very similar spectra (see Supporting Information for details). Hence, the polarity of the solvents has no significant influence on the absorption maxima of diazadibora **7a**. The UV/Vis spectra of the diazadibora derivatives **7b–h** are congruent with the spectra of **7a** (see Supporting Information for details). Furthermore, we also measured the emission spectra of **7a** (dotted black line) and for comparison also of the carbon analogue benzo[*b*]triphenylene (dotted red line). For the diazadibora **7a** we observed a red-shifted emission band ($\lambda_{em.}=494$ & 580 nm) after excitation at 350 nm in comparison to the carbon analog, exhibiting an unusual large Stokes shift of 144 (1.0 eV) and 230 nm (1.4 eV).

The emission intensity of **7a** at 580 nm correlates linearly with the concentration range from 1.0×10^{-5} to 5.0×10^{-5} M.

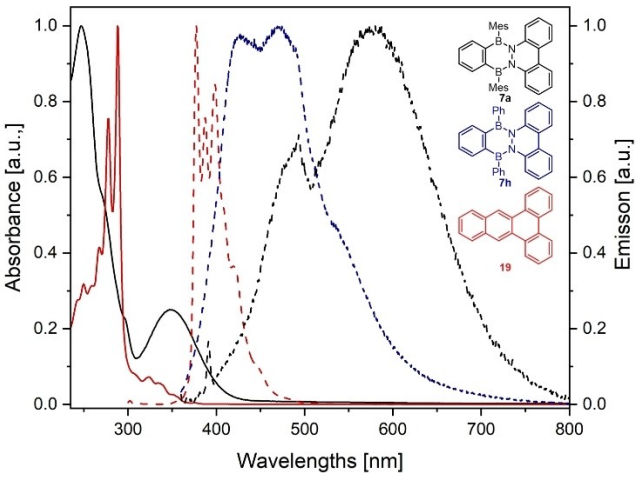

Figure 2. Comparison of the absorption and emission spectra of the mesitylated diazadiborabenzo[*b*]triphenylene **7a** and benzo[*b*]triphenylene (**19**). UV/Vis spectra of the mesitylated diazadiborabenzo[*b*]triphenylene **7a** (solid black line) and benzo[*b*]triphenylene (**19**) (solid red line) both in a concentration of 2.0×10^{-5} M in DCM. The emission spectra of the diazadiborabenzo[b]triphenylene **7a** (dotted black line) and **7h** (dotted blue line) excited ar 350 nm in a concentration of 5.0×10^{-4} M in DCM, and benzo[*b*]triphenylene (**19**) (dotted red line) excited at 277 nm (2.5×10^{-6} M in DCM).

© 2023 The Authors. Angewandte Chemie International Edition published by Wiley-VCH GmbH

15213773, 2023, 15, Downloaded from https://onlinelibrary.wiley.com/doi/10.1002/anie.202300785 by Cochrane Germany, Wiley Online Library on [07/12/2023]. See the Terms and Conditions (https://onlinelibrary.wiley.com/terms-and-conditions) on Wiley Online Library for rules of use; OA articles are governed by the applicable Creative Commons License

However, at higher concentrations this relationship does not hold true (see Supporting Information for details) indicating concentration-dependent quenching. The unchanged emission profile at lower concentrations does not indicate excimer formation.[27] Furthermore, we also investigated the emission in different solvents with different polarities (see Supporting Information for details), such as THF, DCM, cyclohexane and *n*-hexane, and compared them at a concentration of 5.0×10^{-5} M and an excitation wavelength of 350 nm. The lowest emission intensity was observed in THF. With decreasing polarity of the solvent, the emission intensity increased with the highest emission observed in *n*-hexane. However, the wavelength of the emission maxima did not change with different solvent polarity. This observation indicates that the dipole moment within the molecules are relatively small due to competing effects of the B–N π-bonding and the difference in electronegativity. Also, the quantum yield was determined to be $\Phi_F = 0.3\,\%$ for the diazadibora benzo[*b*]triphenylene **7a** in cyclohexane (see Supporting Information for details).

The diazadiboracompounds **7b–h** differ in their photophysical properties from **7a**. The results are summarized in Table 1. All spectra were measured at a concentration of 5.0×10^{-4} M in DCM and excited at 300 or 350 nm. Upon excitation with 350 nm, the emission sprectra of **7b–h** exhibit maxima from 422 to 474 nm and only **7h** shows a dual emission band (Figure 2 – dotted blue line). Quantum yields between 1.0 and 8.1 % in cyclohexane could be observed for **7b–h** (see Supporting Information for details), which are considerably higher than for **7a**. After excitation at 300 nm, the emission maxima of **7b–h** range from 328 to 480 nm. Additionally, **7c** & **7d** have three emission maxima. But none of them has a large Stokes shift as **7a**.

This observation could be due to the twisted $C_2B_2N_2$ core of **7a** (see crystal structure - Figure 3). The steric hinderance of the mesityl groups prevents the core of **7a** to be flat and may thus also inhibit the photochemical relaxation pathway. This is in agreement with the studies of Lu et al. in 2019,[16] who showed that, the large Stokes shift is due to the twisting of the $C_2B_2N_2$ core in the diazadiboranapthalenes **6** in the excited state, which can be prevented in different matrices. Interestingly, our phosphorescence measurements showed a short-lived phosphorescence of all diazadiboratriphenyles **7a–h** between 12.5 and 15.0 msec (see Supporting Information for details). Additionally, the emission of **7a–h** can also be triggered with excitation wavelengths of 302 and 365 nm (see Supporting Information for details). Addionally, we monitored the emission processes of **7a–h** depending on exciation wavelengths of 300, 350, 380 and 400 nm. Herein, it could be shown that depending on the substitution on the boron-atom individual emission parthways are preffered with increasing excitation wavelengths (see Supporting Information for details).

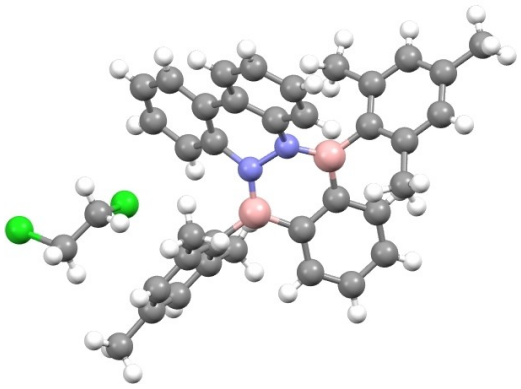

Figure 3. Experimental crystal structure of the diazadibora **7a** crystallized with 1,2-dichloroethane (CCDC 2204514).

Quantum chemical calculations at the DFT/CAM-B3LYP level showed a good agreement between the computed ground-state equilibrium structure and the experimental crystal structure (Figure 3) with bond lengths varying by less than 0.01 Å and dihedral angles by less than 2°.[28] Subsequent calculations of the excited electronic states at TDDFT/CAM-B3LYP level yielded a computed UV/Vis spectrum (Figure 4), which also resembles the experimental one closely, albeit being blue shifted by approx. 0.5 eV due to missing solvation and vibronic effects.

The first peak of the UV/Vis spectrum consists of the first two singlet excited states S_1 (4.11 eV) and S_2 (4.29 eV). The corresponding detachment and attachment densities (Figure 5) characterize both as ππ* excitations, in which electron density is transferred from the central BN building block to the outer π systems of the central building block. The energetically lowest-lying triplet excited state T_1 has an excitation energy of 3.25 eV and corresponds to a ππ* excitation within the biphenylic building block of the central moiety (see Figure 5). Excitation energies and the corresponding detachment and attachment densities of energeti-

Table 1: Overview of the photophysical properties of **7a–h** excited at 300 and 350 nm in DCM, and the corresponding quantum yields of **7a–h** in cyclohexane.

Compound	Emission maxima ex. 300 nm [nm]	Emission maxima ex. 350 nm [nm]	Quantum Yield Φ_F [%]
7a	420, 490 & 560	494 & 580	0.3
7b	427	480	1.0
7c	328, 376 & 480	480	2.2
7d	340, 378 & 486	420	3.4
7e	381	478	4.2
7f	381	432	2.4
7g	416	441	8.1
7h	422	422 & 474	2.8

© 2023 The Authors. Angewandte Chemie International Edition published by Wiley-VCH GmbH

15213773, 2023, 15, Downloaded from https://onlinelibrary.wiley.com/doi/10.1002/anie.202300785 by Cochrane Germany, Wiley Online Library on [07/12/2023]. See the Terms and Conditions (https://onlinelibrary.wiley.com/terms-and-conditions) on Wiley Online Library for rules of use; OA articles are governed by the applicable Creative Commons License

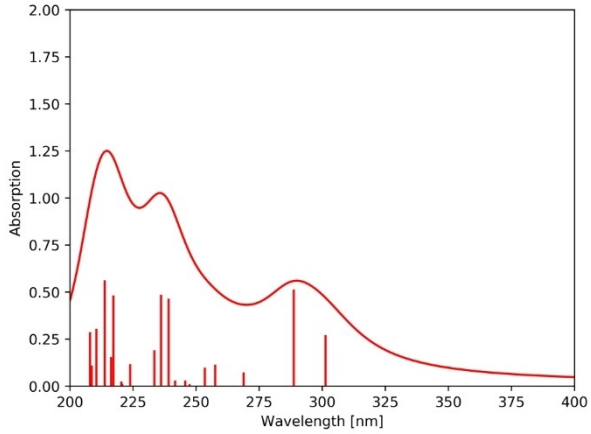

Figure 4. Computed UV/Vis absorption spectrum of the diazadiboraacene **7a**.

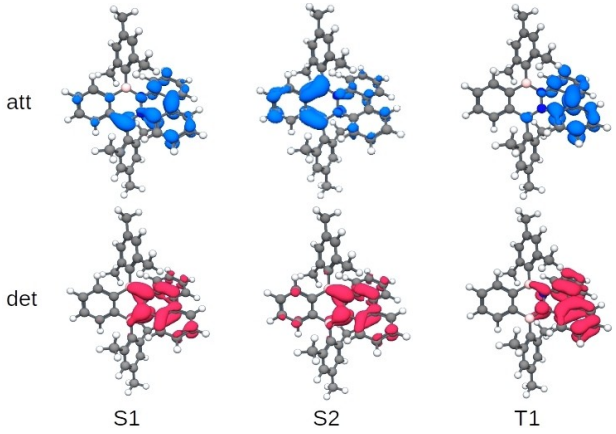

Figure 5. Detachment and attachment densities of the S_1, S_2 and T_1 of the diazadiboraacene **7a** at the ground-state equilibrium geometry.

cally higher-lying states are given in the Supporting Information.

Further investigations showed a good agreement between the computed phosphorescence energy of 2.29 eV corresponding to an emission wavelength of 541 nm and λ_{max} of the experimental phosphorescence band at 575 nm. For this objective, the vertical decay energy has been computed at the equilibrium geometry of the T_1 state. To rationalize the occurrence of phosphorescence, possible intersystem crossing pathways from the singlet into the triplet state manifold need to be considered. According to Fermi's Golden rule, crossing rates are particularly high at points of state crossings, where the singlet and triplet states are energetically degenerate. Then ISC rates can be large despite small spin-orbit coupling elements.

Upon photoexcitation and internal conversion, the S_1 state is populated at the equilibrium geometry of the ground state, i.e. the Franck–Condon point on the S_1 surface. At this geometry, six triplet excited states are found to lie energetically below the S_1 state. During relaxation into its equilibrium geometry, the S_1 drops drastically in energy, and at the S1 equilibrium geometry only one triplet state is found energetically lower than S_1 (Table 2). In other words, the PES of the S_1 crosses those of five triplet states during the initial relaxation. As described above, each of these singlet-triplet crossings allow in principle for ISC into the triplet manifold even though the spin-orbit coupling elements are small at TDDFT level computed at the Franck–Condon geometry as well as at the relaxed S_1 geometry. Once arrived in the triplet manifold, the molecules will continue to relax into the T_1 minimum and decay via the observed phosphorescence.

Additionally, the diazadiboratriphenylene **7a** was electrochemically characterized and cyclic voltammetry measurements in DCM showed an irreversible oxidation wave at +1.31 (vs SCE). During CV measurements, no reduction wave was observed (see Supporting Information for details).

In summary, we presented a novel synthetic strategy to access diazadiborabenzo[*b*]triphenylene **7a–h** via biradical **16** as key intermediate. Thereby, we exploited the equilibrium of the coordination of the second benzo[*c*]cinnoline (**15**) of the biradical **16**. By addition of Grignard reagents **18a–h**, we were able to successfully access the diazadiborabenzo[*b*]triphenylene **7a–h**. We investigated the absorption, emission and excitation spectra of the novel diazadiboraacene **7a–h**. In contrast to diazadiboratriphenylene derivatives **5** from Jaska et al., which shows mainly a yellow-orange emission with maxima between 521 and

Table 2: Excitation energies for the lowest excited states of **7a** computed at the equilibrium geometries of the electronic ground state S_0, and the first excited singlet and triplet states S_1 and T_1, respectively.

S_0 eq. geometry		S_1 eq. geometry		T_1 eq. geometry	
State	ω [eV]	State	ω [eV]	State	ω [eV]
T_1	3.25	T_1	1.84	T_1	2.29
T_2	3.53	S_1	2.20	T_2	3.05
T_3	3.72	T_2	2.70	S_1	3.24
T_4	3.86	T_3	3.23	T_3	3.53
T_5	3.88	T_4	3.35	T_4	3.75
T_6	4.05	S_2	3.38	S_2	3.76
S_1	4.12	T_5	3.55	T_5	3.84
T_7	4.18	T_6	3.60	T_6	3.87
T_8	4.20	S_3	3.78	T_7	3.92
S_2	4.29	T_7	3.86	T_8	3.99

© 2023 The Authors. Angewandte Chemie International Edition published by Wiley-VCH GmbH

15213773, 2023, 15, Downloaded from https://onlinelibrary.wiley.com/doi/10.1002/anie.202300785 by Cochrane Germany, Wiley Online Library on [07/12/2023]. See the Terms and Conditions (https://onlinelibrary.wiley.com/terms-and-conditions) on Wiley Online Library for rules of use; OA articles are governed by the applicable Creative Commons License

586 nm, we could show that the diazadiborabenzo-[*b*]triphenylene **7a**–**h** have mainly a blue or green emission with maxima between 328 and 494 nm.[14] The quantum yields are in a similar range like those of diazadiboratriphenylene derivatives **5**. Only the quantum yield of **7a**, which has a similar emission maximum as **5**, is lower. In comparison with the azaboraanthracence **3**, which has an emission maximum of 447 nm, we could show that a larger dipole moment in the molecule does in general not lead to a larger Stokes shift.[12] We could demonstrate that small changes at the boron-attached aryl-ring can have a significant influence on the emission properties. Additionally, the emission could be assigned to short life-time phosphorescence. The exact relaxation of the different derivates **7a**–**h** will be investigated in future studies. In conclusion, we synthesized novel B,N benzo[*b*]triphenylenes with tunable emission properties via a highly modular synthetic route, giving access to a new class of B,N-PAHs with promising potential as molecular materials.

Acknowledgements

The authors thank the DFG for funding, Heike Hausmann (Justus Liebig University, Giessen) for NMR-measurements, Frederik R. Erb (Justus Liebig University, Giessen) for CV measurements and Michel Große (Justus Liebig University, Giessen) for X-Ray analysis. Open Access funding enabled and organized by Projekt DEAL.

Conflict of Interest

The authors declare no conflict of interest.

Data Availability Statement

The data that support the findings of this study are available in the supplementary material of this article.

Keywords: Acenes · Boron · Nitrogen · Phosphorescence · Polycycles

[1] a) R. Freudenmann, B. Behnisch, M. Hanack, *J. Mater. Chem.* **2001**, *11*, 1618–1624; b) G. Albrecht, C. Geis, J. M. Herr, J. Ruhl, R. Göttlich, D. Schlettwein, *Org. Electron.* **2019**, *65*, 321–326; c) I. Seguy, P. Jolinat, P. Destruel, J. Farenc, R. Mamy, H. Bock, J. Ip, T. P. Nguyen, *J. Appl. Phys.* **2001**, *89*, 5442–5448.

[2] a) D. Adam, F. Closs, T. Frey, D. Funhoff, D. Haarer, P. Schuhmacher, K. Siemensmeyer, *Phys. Rev. Lett.* **1993**, *70*, 457–460; b) D. Adam, P. Schuhmacher, J. Simmerer, L. Häussling, K. Siemensmeyer, K. H. Etzbachi, H. Ringsdorf, D. Haarer, *Nature* **1994**, *371*, 141–143.

[3] M. Oukachmih, P. Destruel, I. Seguy, G. Ablart, P. Jolinat, S. Archambeau, M. Mabiala, S. Fouet, H. Bock, *Sol. Energy Mater. Sol. Cells* **2005**, *85*, 535–543.

[4] a) M. D. Watson, A. Fechtenkötter, K. Müllen, *Chem. Rev.* **2001**, *101*, 1267–1300; b) J. Wu, W. Pisula, K. Müllen, *Chem. Rev.* **2007**, *107*, 718–747; c) M. Bendikov, F. Wudl, D. F. Perepichka, *Chem. Rev.* **2004**, *104*, 4891–4946.

[5] P. G. Campbell, A. J. V. Marwitz, S.-Y. Liu, *Angew. Chem. Int. Ed.* **2012**, *51*, 6074–6092; *Angew. Chem.* **2012**, *124*, 6178–6197.

[6] a) C. Mützel, J. M. Farrell, K. Shoyama, F. Würthner, *Angew. Chem. Int. Ed.* **2022**, *61*, e202115746; *Angew. Chem.* **2022**, *134*, e202115746; b) Q. Shi, X. Shi, C. Feng, Y. Wu, N. Zheng, J. Liu, X. Wu, H. Chen, A. Peng, J. Li et al, *Angew. Chem. Int. Ed.* **2021**, *60*, 2924–2928; *Angew. Chem.* **2021**, *133*, 2960–2964; c) A. John, S. Kirschner, M. K. Fengel, M. Bolte, H.-W. Lerner, M. Wagner, *Dalton Trans.* **2019**, *48*, 1871–1877.

[7] a) Z. Liu, T. B. Marder, *Angew. Chem. Int. Ed.* **2008**, *47*, 242–244; *Angew. Chem.* **2008**, *120*, 248–250; b) T. Lorenz, M. Crumbach, T. Eckert, A. Lik, H. Helten, *Angew. Chem. Int. Ed.* **2017**, *56*, 2780–2784; *Angew. Chem.* **2017**, *129*, 2824–2828; c) X. Chen, D. Tan, D.-T. Yang, *J. Mater. Chem. C* **2022**, *10*, 13499–13532; d) H. Gotoh, S. Nakatsuka, H. Tanaka, N. Yasuda, Y. Haketa, H. Maeda, T. Hatakeyama, *Angew. Chem. Int. Ed.* **2021**, *60*, 12835–12840; *Angew. Chem.* **2021**, *133*, 12945–12950; e) T. Kaehler, M. Bolte, H.-W. Lerner, M. Wagner, *Angew. Chem. Int. Ed.* **2019**, *58*, 11379–11384; *Angew. Chem.* **2019**, *131*, 11501–11506; f) M. Krieg, F. Reicherter, P. Haiss, M. Ströbele, K. Eichele, M.-J. Treanor, R. Schaub, H. F. Bettinger, *Angew. Chem. Int. Ed.* **2015**, *54*, 8284–8286; *Angew. Chem.* **2015**, *127*, 8402–8404; g) M. Müller, S. Behnle, C. Maichle-Mössmer, H. F. Bettinger, *Chem. Commun.* **2014**, *50*, 7821–7823; h) G. Bélanger-Chabot, H. Braunschweig, D. K. Roy, *Eur. J. Inorg. Chem.* **2017**, 4353–4368; i) A. Maiti, B. J. Elvers, S. Bera, F. Lindl, I. Krummenacher, P. Ghosh, H. Braunschweig, C. B. Yildiz, C. Schulzke, A. Jana, *Chem. Eur. J.* **2022**, *28*, e202104567; j) A. S. Scholz, J. G. Massoth, M. Bursch, J.-M. Mewes, T. Hetzke, B. Wolf, M. Bolte, H.-W. Lerner, S. Grimme, M. Wagner, *J. Am. Chem. Soc.* **2020**, *142*, 11072–11083; k) M. R. Rapp, W. Leis, F. Zinna, L. Di Bari, T. Arnold, B. Speiser, M. Seitz, H. F. Bettinger, *Chem. Eur. J.* **2022**, *28*, e202104161; l) M. Fingerle, C. Maichle-Mössmer, S. Schundelmeier, B. Speiser, H. F. Bettinger, *Org. Lett.* **2017**, *19*, 4428–4431; m) M. Stępień, E. Gońka, M. Żyła, N. Sprutta, *Chem. Rev.* **2017**, *117*, 3479–3716.

[8] M. J. S. Dewar, V. P. Kubba, R. Pettit, *J. Chem. Soc.* **1958**, 3073–3076.

[9] a) M. J. S. Dewar, R. Dietz, *J. Org. Chem.* **1961**, *26*, 3253–3256; b) S. S. Chissick, M. Dewar, P. M. Maitlis, *Tetrahedron Lett.* **1960**, *1*, 8–10; c) F. A. Davis, M. Dewar, R. Jones, S. D. Worley, *J. Am. Chem. Soc.* **1969**, *91*, 2094–2097; d) M. J. S. Dewar, P. M. Maitlis, *J. Am. Chem. Soc.* **1961**, *83*, 187–193; e) M. Dewar, V. P. Kubba, *Tetrahedron* **1959**, *7*, 213–222; f) M. Dewar, R. Jones, *J. Am. Chem. Soc.* **1968**, *90*, 2137–2144; g) M. Dewar, R. Dietz, V. P. Kubba, A. R. Lepley, *J. Am. Chem. Soc.* **1961**, *83*, 1754–1756; h) M. Dewar, G. J. Gleicher, B. P. Robinson, *J. Am. Chem. Soc.* **1964**, *86*, 5698–5699; i) M. Dewar, V. P. Kubba, *J. Am. Chem. Soc.* **1961**, *83*, 1757–1760.

[10] a) T. Hasegawa, J. Takeya, *Sci. Technol. Adv. Mater.* **2009**, *10*, 024314; b) T. Hatakeyama, S. Hashimoto, S. Seki, M. Nakamura, *J. Am. Chem. Soc.* **2011**, *133*, 18614–18617; c) J. E. Anthony, *Chem. Rev.* **2006**, *106*, 5028–5048; d) J. E. Anthony, *Angew. Chem. Int. Ed.* **2008**, *47*, 452–483; *Angew. Chem.* **2008**, *120*, 460–492; e) M. J. D. Bosdet, W. E. Piers, T. S. Sorensen, M. Parvez, *Angew. Chem. Int. Ed.* **2007**, *46*, 4940–4943; *Angew. Chem.* **2007**, *119*, 5028–5031.

[11] J. S. A. Ishibashi, J. L. Marshall, A. Mazière, G. J. Lovinger, B. Li, L. N. Zakharov, A. Dargelos, A. Graciaa, A. Chrostowska, S.-Y. Liu, *J. Am. Chem. Soc.* **2014**, *136*, 15414–15421.

[12] D. Tian, G. Shi, M. Fan, X. Guo, Y. Yuan, S. Wu, J. Liu, J. Zhang, S. Xing, B. Zhu, *Org. Lett.* **2021**, *23*, 8163–8168.

© 2023 The Authors. Angewandte Chemie International Edition published by Wiley-VCH GmbH

15213773, 2023, 15, Downloaded from https://onlinelibrary.wiley.com/doi/10.1002/anie.202300785 by Cochrane Germany, Wiley Online Library on [07/12/2023]. See the Terms and Conditions (https://onlinelibrary.wiley.com/terms-and-conditions) on Wiley Online Library for rules of use; OA articles are governed by the applicable Creative Commons License

[13] a) W. Siebert, R. Full, H. Schmidt, J. von Seyerl, M. Halstenberg, G. Huttner, *J. Organomet. Chem.* **1980**, *191*, 15–25; b) H. Schmidt, W. Siebert, *J. Organomet. Chem.* **1978**, *155*, 157–163.
[14] C. A. Jaska, D. J. H. Emslie, M. J. D. Bosdet, W. E. Piers, T. S. Sorensen, M. Parvez, *J. Am. Chem. Soc.* **2006**, *128*, 10885–10896.
[15] M. J. Bosdet, W. E. Piers, T. S. Sorensen, M. Parvez, *Can. J. Chem.* **2010**, *88*, 426–433.
[16] Z. Lu, H. Quanz, J. Ruhl, G. Albrecht, C. Logemann, D. Schlettwein, P. R. Schreiner, H. A. Wegner, *Angew. Chem. Int. Ed.* **2019**, *58*, 4259–4263; *Angew. Chem.* **2019**, *131*, 4303–4307.
[17] Z. Lu, H. Quanz, O. Burghaus, J. Hofmann, C. Logemann, S. Beeck, P. R. Schreiner, H. A. Wegner, *J. Am. Chem. Soc.* **2017**, *139*, 18488–18491.
[18] Z. Zhou, A. Wakamiya, T. Kushida, S. Yamaguchi, *J. Am. Chem. Soc.* **2012**, *134*, 4529–4532.
[19] a) C. Reus, S. Weidlich, M. Bolte, H.-W. Lerner, M. Wagner, *J. Am. Chem. Soc.* **2013**, *135*, 12892–12907; b) T. Agou, M. Sekine, T. Kawashima, *Tetrahedron Lett.* **2010**, *51*, 5013–5015.
[20] V. M. Hertz, N. Ando, M. Hirai, M. Bolte, H.-W. Lerner, S. Yamaguchi, M. Wagner, *Organometallics* **2017**, *36*, 2512–2519.
[21] a) H. F. Bettinger, M. Filthaus, *J. Org. Chem.* **2007**, *72*, 9750–9752; b) D. Kaufmann, *Chem. Ber.* **1987**, *120*, 901–905.
[22] S. Bader, S. Kessler, H. Wegner, *Synthesis* **2010**, *2010*, 2759–2762.
[23] a) H. Eriksson, M. Håkansson, *Organometallics* **1997**, *16*, 4243–4244; b) M. Schlosser, V. Ladenberger, *J. Organomet. Chem.* **1967**, *8*, 193–197; c) G. Costa, A. Camus, L. Gatti, N. Marsich, *J. Organomet. Chem.* **1966**, *5*, 568–572.
[24] a) D. Wu, L. Kong, Y. Li, R. Ganguly, R. Kinjo, *Nat. Commun.* **2015**, *6*, 7340; b) M.-A. Légaré, G. Bélanger-Chabot, R. D. Dewhurst, E. Welz, I. Krummenacher, B. Engels, H. Braunschweig, *Science* **2018**, *359*, 896–900; c) B. Wang, Y. Li, R. Ganguly, H. Hirao, R. Kinjo, *Nat. Commun.* **2016**, *7*, 11871.
[25] a) C. K. Narula, H. Noeth, *Inorg. Chem.* **1985**, *24*, 2532–2539; b) U. Höbel, H. Nöth, H. Prigge, *Chem. Ber.* **1986**, *119*, 325–337.
[26] Ö. Seven, Z.-W. Qu, H. Zhu, M. Bolte, H.-W. Lerner, M. C. Holthausen, M. Wagner, *Chem. Eur. J.* **2012**, *18*, 11284–11295.
[27] H. Saigusa, E. C. Lim, *Acc. Chem. Res.* **1996**, *29*, 171–178.
[28] T. Yanai, D. P. Tew, N. C. Handy, *Chem. Phys. Lett.* **2004**, *393*, 51–57.

Manuscript received: January 16, 2023
Accepted manuscript online: February 13, 2023
Version of record online: March 2, 2023

© 2023 The Authors. Angewandte Chemie International Edition published by Wiley-VCH GmbH

15213773, 2023, 15, Downloaded from https://onlinelibrary.wiley.com/doi/10.1002/anie.202300785 by Cochrane Germany, Wiley Online Library on [07/12/2023]. See the Terms and Conditions (https://onlinelibrary.wiley.com/terms-and-conditions) on Wiley Online Library for rules of use; OA articles are governed by the applicable Creative Commons License